

Received April 22, 2019, accepted May 20, 2019, date of publication June 5, 2019, date of current version June 21, 2019.

Digital Object Identifier 10.1109/ACCESS.2019.2920932

Machine Learning-Based Lithium-Ion Battery Capacity Estimation Exploiting Multi-Channel Charging Profiles

YOHWAN CHOI, SEUNGHYOUNG RYU^{ID}, KYUNGNAM PARK,
AND HONGSEOK KIM^{ID}, (Senior Member, IEEE)

Department of Electronic Engineering, Sogang University, Seoul 04107, South Korea

Corresponding author: Hongseok Kim (hongseok@sogang.ac.kr)

This work was supported by the Basic Science Research Program through the National Research Foundation of Korea (NRF) funded by the Ministry of Science and ICT under Grant NRF-2017R1A1A1A05001377.

ABSTRACT Prognostics and health management is a promising methodology to cope with the risks of failure in advance and has been implemented in many well-known applications including battery systems. Since the estimation of battery capacity is critical for safe operation and decision making, battery capacity should be estimated precisely. In this regard, we leverage measurable data such as voltage, current, and temperature profiles from the battery management system whose patterns vary in cycles as aging. Based on these data, the relationship between capacity and charging profiles is learned by neural networks. Specifically, to estimate the state of health accurately we apply feedforward neural network, convolutional neural network, and long short-term memory. Our results show that the proposed multi-channel technique based on voltage, current, and temperature profiles outperforms the conventional method that uses only voltage profile by up to 25%–58% in terms of mean absolute percentage error.

INDEX TERMS Lithium-ion battery, neural network, remaining useful life, capacity estimation, state of health.

I. INTRODUCTION

Prognostics and health management (PHM) has been used to cope with potential failures in many well-known applications such as utility networks, aerospace, manufacturing, etc. [1], [2]. If it is possible to predict when failure occurs, we can take proper actions proactively for reliable system operation. In addition, PHM predicts the degradation of components *just in time* and thus conventional maintenance paradigm can be simplified. In doing this remaining useful life (RUL) is defined as a period until the limit for safe criterion of component or system is reached. It is essential to estimate the state of system with high reliability from the perspectives of stable operation against failure. According to the ISO 13381-1, prognostic is defined as “the analysis of the symptoms of faults to predict future condition and residual life within design parameters” [3].

In general, lithium-ion battery has been widely used in many applications such as cell phones, electric vehicles, and

The associate editor coordinating the review of this manuscript and approving it for publication was Rui Xiong.

energy storage systems due to its long cycle life, high energy and high power densities [4], [5]. One of the essential factors to consider in using battery is the degradation since batteries are still expensive. Thus it is desirable to extend battery lifetime considering battery characteristics. Battery degradation needs to be considered from safety perspectives to prevent explosion or the loss of life. Since the estimation of state of health (SoH) is crucial for user safety and decision making, battery health should be estimated accurately. In addition a battery produces electricity through electrochemical reactions as a power source and total available capacity decreases as the battery is repeatedly charged and discharged. That is, active substances affecting the output power and the available capacity of battery are reduced due to repeated chemical reactions over time as the battery ages, and this results in performance degradation. That is why SoH estimation with high accuracy is extremely important for safe operation, battery replacement and reduction of maintenance cost. Furthermore, in order to prevent critical failure, it is desirable to identify whether the battery operates in an abnormal condition.

So far, there have been many studies about SoH estimation and RUL prediction, which can be categorized into two cases: model-based, e.g., electrochemical model and equivalent circuit model (ECM) vs. data-driven methods. As an electrochemical model, Goebel *et al.* [6] estimate the capacity through negative linear relationship between capacity and internal impedance by measuring the internal impedance of battery via electrochemical impedance spectrometry technique. In [7], Daigle and Kulkarni establish an aging model of batteries during discharging based on electrochemical-based model to predict active lithium-ion parameters, internal impedance and diffusion constant, then derive capacity as a result. In addition, a single-particle model with several refined parameters was also derived to investigate capacity degradation sources of a graphite/LiFePO₄ cell in both storage and cycling conditions [8]. Although these methods give a fundamental understanding and interpretation of spatio-temporal dynamics of electrochemical reactions inside battery, they are yet practical due to computational complexity resulted from solving many partial differential equations. ECM has relatively low computational complexity compared to the electrochemical model, but is only applicable to limited operating conditions when parameters have been identified.

Recently, to overcome the drawbacks of the above approaches, data-driven methods are gaining remarkable attention as machine learning techniques rapidly advance. Among data-driven methods, the adaptive state estimation approaches, such as unscented particle filter (UPF) [9], unscented Kalman filter [10] and particle filter [11], [12], have been used for real time prediction of battery RUL. In [13], Zheng and Fang proposed a framework based on relevance vector regression to simulate lithium-ion battery RUL and short-term capacity prediction. Then, unscented Kalman filter was utilized to estimate the battery parameters for predicting RUL recursively. Similarly, particle filter was used for predicting RUL and the time until the end of discharge voltage in [12]. However, they still require an accurate battery model.

Another data-driven method is based on machine learning techniques such as support vector machine [14], ensemble learning [15], relevance vector machine [16], artificial neural network [17] and long short-term memory (LSTM) [18]. Specifically, Liu *et al.* presented an optimized relevance vector machine algorithm to improve the accuracy and the stability of RUL estimation and to present the uncertainty of RUL estimation [16]. In [17], feedforward neural network (FNN) is used to calculate the RUL through sampled voltage data. Very recently, You *et al.* [18] show that voltage and current changes in time can be learned by LSTM to predict capacity decrease, but it is more complex than other machine learning based methods. In [19], Hu *et al.* exploit the combination of sample entropy and the advanced sparse Bayesian predictive modeling to establish the underlying relationship between the sample entropy and the capacity loss. In doing this, the input data are constructed by the sample entropy of short voltage sequence from hybrid pulse power characterization

test at three different temperatures. By contrast, the proposed method directly uses the multi-channel charging profiles of voltage, current and surface temperature as an input data, which leads to different machine learning models from [19]. In overall, data-driven methods can reflect the inherent characteristics of aging without knowing the electrochemical principles of battery, and thus are easy to implement, computationally inexpensive and less complex than model-based methods. In this paper we further develop the data-driven method exploiting multi-channel charging profiles of voltage (V), current (I) and surface temperature of lithium-ion battery (T) in applying machine learning techniques.

We highlight our contributions as follows. We propose a capacity estimation framework for lithium-ion battery based on multi-channel machine learning techniques using FNN, convolutional neural network (CNN) and LSTM, respectively, and show that utilizing the diversity of feasible data substantially improves estimation accuracy. In terms of learning methodologies, LSTM shows the best performance, followed by FNN and CNN in order; the selection of learning method depends on the tradeoff between model complexity and target estimation error. LSTM is preferred as long as the model complexity is acceptable from computational power and/or the available datasets. Based on lithium-ion battery dataset obtained from NASA [20], we evaluate the estimation errors and the capacity difference per cycle. Numerical results demonstrate that the proposed multi-channel method achieves up to 58%, 46% and 25% of MAPE improvement in the case of FNN, CNN and LSTM, respectively, compared to using voltage charging profiles only.

The remainder of this paper is organized as follows. In Section II, we present the system model and describe the characteristics of battery data sets. In Section III we propose machine learning based SoH estimation techniques using FNN, CNN and LSTM. Extensive experiment results along with learning methodologies and battery types are presented in Section IV, followed by conclusion in Section V.

II. SYSTEM MODEL

A. MOTIVATION

To motivate our work, we present Fig. 1 as an illustration of PHM; as human ages, there are several noticeable changes such as wrinkles of the face and depth, skin elasticity, hair condition, etc. Then it is possible to estimate the age of a person by fully exploiting these external changes. In the case of bearings, one can estimate the failure time when faults occur by observing cracks, spalls on a surface, and changes in vibration signals. Inspired by this principle, we come up with the idea of estimating battery health by using feasible data such as voltage, current and surface temperature (or simply called temperature hereafter), which are typically provided by battery management system (BMS).

B. LITHIUM-ION BATTERY DATA OF NASA

We use battery data sets provided by NASA Prognostics Center of Excellence Data Repository [20], and these data sets consist of eight lithium-ion batteries that run through

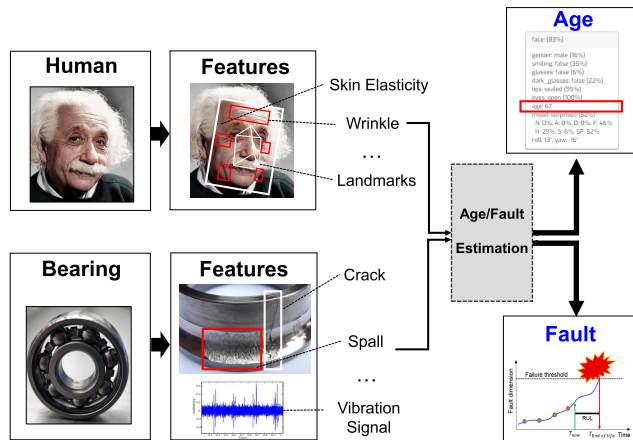


FIGURE 1. An illustration of PHM for aging estimation.

three different operational profiles, i.e., charging, discharging and rest period, at room temperature. The experiments consist of applying the repeated charging and discharging cycles to commercially available 18650 lithium-ion cells for achieving accelerated aging. Batteries are charged by the constant current constant voltage (CCCV) principle; charging at constant current of 1.5 A until the voltage reaches the cell upper voltage limit of 4.2 V, then applying constant voltage until the current drops to 20 mA. Discharging is done at the constant current of 2 A until the cell voltage falls to 2.7 V, 2.5 V, 2.2 V, and 2.5 V for batteries #5, #6, #7, and #18, respectively. The experiments are performed until the batteries lose 30% of the rated capacity, i.e., 1.4 Ah. Additional electrochemical impedance data are also provided in this dataset, but not used in our work.

C. DATA ACQUISITION DURING CHARGING PROCESS

To capture how the internal battery parameters changed along the aging, which are critical in estimating battery degradation, we leverage the voltage, current and temperature data; the data is measured at every *charging* cycle. There are three status of battery in actual application: charging, discharging and rest. During discharging process, it is hard to measure or calculate internal parameters precisely since the current rapidly changes in time. According to recent works [21], [22], there is a re-balancing process of active materials and relaxation of gradients generated due to the passage of current in the rest period, which would enable capacity regeneration. For this reason, the internal battery parameters are generally constant or change slowly compared to the charging or discharging period, which makes the estimation of internal parameters difficult since they cannot be calculated based on the amount of indistinctive data [17]. However, batteries usually have a peaceful charging process based on preset protocols in which the necessary external electrical performance can be easily measured. Furthermore, since discharging pattern mainly depends on the owner's routine with high randomness, it is much easier to utilize battery charging profiles.

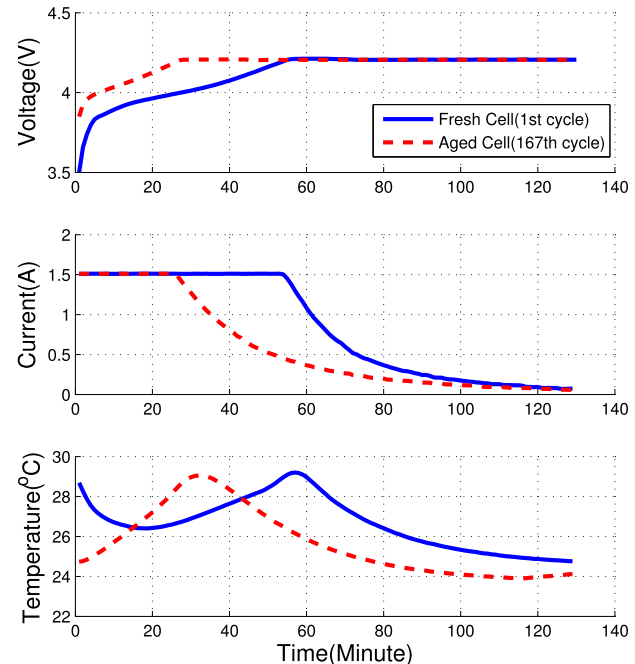


FIGURE 2. Voltage, current and temperature charging profiles for fresh cell and aged cell: Battery #5 from NASA battery set.

D. MULTI-CHANNEL CHARGING PROFILES OF V, I, T DATA

In Fig. 2, we observe that there are significant changes in charging profiles of voltage, current and temperature as a battery ages; the voltage of aged cell during charging process reaches 4.2 V earlier than that of fresh cell, and the current of aged cell begins to drop from constant current earlier than the fresh cell. Moreover, the aged cell reaches the maximum temperature earlier than the fresh cell. The reason why the beginnings of temperature profiles of the first and the 167th cycle are different is due to the repeated process of charging, rest and discharging. Since the temperature at the end of discharging usually rises compared to that of the beginning, this affects the initial temperature of the next charging profile. To quantify the battery aging, we need to define the SoH properly. Even though there is no unified way to define SoH, it is commonly defined using capacity as given by

$$\text{SoH}(\%) = \frac{C_k}{C_0} \times 100 \quad (1)$$

where C_0 is the rated capacity and C_k is the measured capacity at cycle k . In addition, we determine that battery life is over when the measured capacity is below 70% of the rated capacity, under which reliable performance cannot be guaranteed.

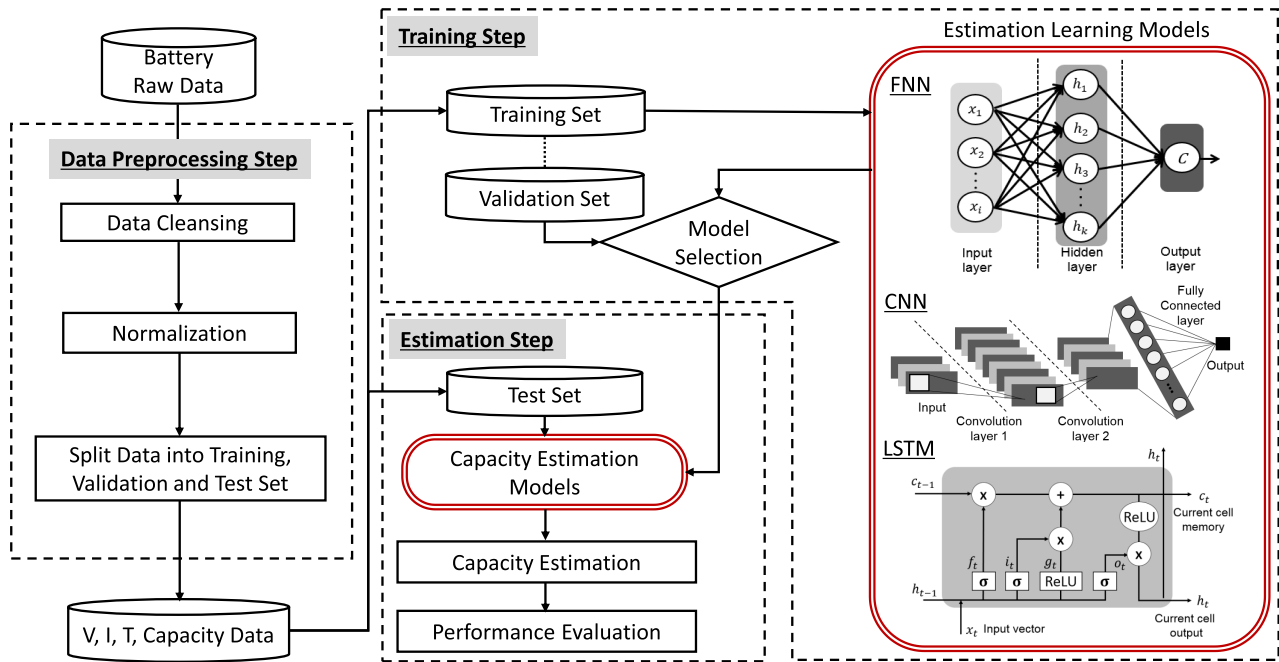
III. MACHINE LEARNING BASED APPROACHES

A. PROPOSED FRAMEWORK

In Fig. 3, we overview the proposed framework for estimating battery capacity exploiting multi-channel charging profiles based on FNN, CNN and LSTM. This framework consists of three steps: data preprocessing, training, and estimation. In step 1, abnormal data is removed by applying data

TABLE 1. Specification of batteries of NASA prognostics center of excellence data repository.

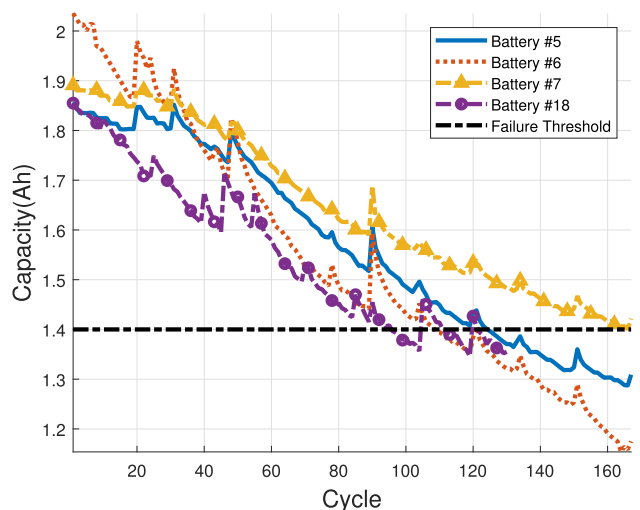
Battery no.	Charging			Discharging		Operating conditions		
	Constant current (A)	Upper voltage limit (V)	Cut-off current (mA)	Constant current (A)	Cut-off voltage (V)	Operating temperature	Initial capacity (Ah)	End of Life (EoL) criteria (Ah)
Battery #5	1.5	4.2	20	2	2.7	Room temp.	1.86	1.40
Battery #6	1.5	4.2	20	2	2.5	Room temp.	2.04	1.40
Battery #7	1.5	4.2	20	2	2.2	Room temp.	1.89	1.40
Battery #18	1.5	4.2	20	2	2.5	Room temp.	1.86	1.40

**FIGURE 3.** An overall framework of the proposed capacity estimation.

cleansing and min-max normalization. Then, the data set is divided into training, validation and test sets. Finally we get the refined voltage, current, temperature, and capacity data. In step 2, training and validation sets are utilized to select a proper model based on FNN, CNN and LSTM, respectively. In step 3, by using capacity estimation models that are determined in the previous step, we estimate the battery capacity and evaluate the performance of the proposed methods.

B. DATA PREPROCESSING

Before utilizing battery data set as experimental data, we preprocess data by removing outliers and securing available data. Eventually, we obtain four sets of battery data with degradation characteristics per cycle as shown in Fig. 4; batteries #5, #6, #7, and #18 (following the numbering of the online repository in [20]) are chosen for the experiment. The overall specification of batteries and charging/discharging conditions are summarized in Table 1. Meanwhile, even though there are many data points during charging process according to the setting of BMS, it is not efficient to utilize all data due to data sensitivity and complexity in estimation, and thus we use the

**FIGURE 4.** Capacity degradations in cycle.

subsampled data that preserve the apparent changes during the charging interval. The inputs of the proposed models are the extracted features, which are obtained by the uniform

sampling of the raw battery data. Specifically, we configure the input matrix as 30-dimensional vectors by concatenating the V, I, T charging profiles, each with 10 samples. The number of samples is chosen to consider the distinct changes in time and the model complexity. In addition, we average the data over sampling interval to prevent oscillation in short time interval.

We adopt min-max normalization for better training since it retains the original distribution of data except for a scaling factor and transforms all the data into the range of [0,1] as below [23]:

$$z_i^k = \frac{x_i^k - \min(\mathbf{x})}{\max(\mathbf{x}) - \min(\mathbf{x})} \quad i \in \{1, \dots, n\} \quad (2)$$

where \mathbf{x} is a collection of all charging cycles, i.e., $\{x_i^k\}$ and n represents the number of samples per cycle. Obviously, we also adopt denormalization process when presenting the final estimation results.

C. FEEDFORWARD NEURAL NETWORK (FNN)

We first apply feedforward neural network, which is a widely used machine learning method having no feedback connections [24]. FNN consists of multiple layers, and each layer has neurons providing nonlinear activation according to the weighted connections to the previous layer. We use a typical structure of FNN, i.e., one hidden layer considering the variability of input data.

D. CONVOLUTIONAL NEURAL NETWORK (CNN)

We also apply CNN, which is a well-known deep learning architecture that uses convolution instead of general matrix multiplication in at least one of their layers [24]. The operation of 2-dimensional convolution is as follows:

$$S(i, j) = (X * W)(i, j) = \sum_m \sum_n X(i - m, j - n)W(m, n) \quad (3)$$

where X is an input matrix and W is a kernel matrix. The typical structure of CNN consists of convolution layer, pooling layer and fully-connected layer [25]. In the convolution layer, the convolution operation is performed to extract features, and the output is passed to the activation function. The pooling layer can be conducted for the purpose of reducing the spatial size of the feature map and provides robust learning results for input data. The output signal is then passed on to the next layer. By passing through multiple steps of convolution and pooling layers, global features can be obtained from input data. Eventually, classification or regression is achieved through the fully connected layer.

E. LONG SHORT-TERM MEMORY (LSTM)

Recurrent neural network (RNN) is a neural network involving directed cycles in memory and shows outstanding performance especially for sequential data. Due to vanishing gradient problem, the basic RNN structure is vulnerable when the time series data has long term dependency. Thus we

apply LSTM, which is designed to mitigate the vanishing gradient problem [26]. A common LSTM unit is composed of a cell, an input gate, an output gate and a forget gate. The cell remembers values over arbitrary time intervals and three gates regulate the flow of information into and out of the cell. LSTM defines an internal memory cell state to store long-term information. The memory cell state interacts with the previous output and the following input to determine which elements of internal state vector should be updated, maintained, or erased.

F. MODEL SELECTION

We design the structures of FNN, CNN and LSTM using the validation set. Each learning method is implemented by Tensorflow in Python [27] with the Intel i7-7700 CPU of 3.60 GHz and 16 GB memory. The average training time is less than 20 seconds, and the drop-out for regularization is 0.5. We use the mean squared error as a loss function, and the Adam optimizer is used with the learning rate of 0.001 [28]. We set the training epochs as 500 and use the batch size of 50. Leaky ReLU is used as an activation function [29]. To evaluate the estimation accuracy, we adopt the mean absolute percentage error (MAPE) as an representative error index as follows:

$$\text{MAPE}(\%) = \frac{100}{K} \sum_{k=1}^K \frac{|l(k) - \hat{l}(k)|}{l(k)} \quad (4)$$

where $l(k)$ presents the actual capacity, $\hat{l}(k)$ is the estimated value and K is the number of cycles. In addition, we compute the mean absolute error (MAE) and the root mean square error (RMSE) as follows:

$$\text{MAE} = \frac{1}{K} \sum_{k=1}^K |l(k) - \hat{l}(k)|, \quad (5)$$

$$\text{RMSE} = \sqrt{\frac{1}{K} \sum_{k=1}^K (l(k) - \hat{l}(k))^2}. \quad (6)$$

The model structures and hyper-parameters are summarized in Table 2.

IV. PERFORMANCE EVALUATION

A. ESTIMATION RESULTS OF USING V DATA

We first present the result of capacity estimation using only voltage charging profiles with 10 uniformly sampled data point as in [14]. Since the available datasets are limited, we need to fully exploit the available datasets. Thus, out of 4 datasets, we select three battery sets as a training set and the remaining one as a test set, and repeat this process four times to have four test results. Then we average four cases of simulation to evaluate the average performance. Fig. 5 shows the capacity estimation results of FNN, CNN and LSTM. In overall, LSTM shows very accurate capacity estimation, even in the case of battery #18 where FNN and CNN based methods show high fluctuations. Note that FNN-1 with

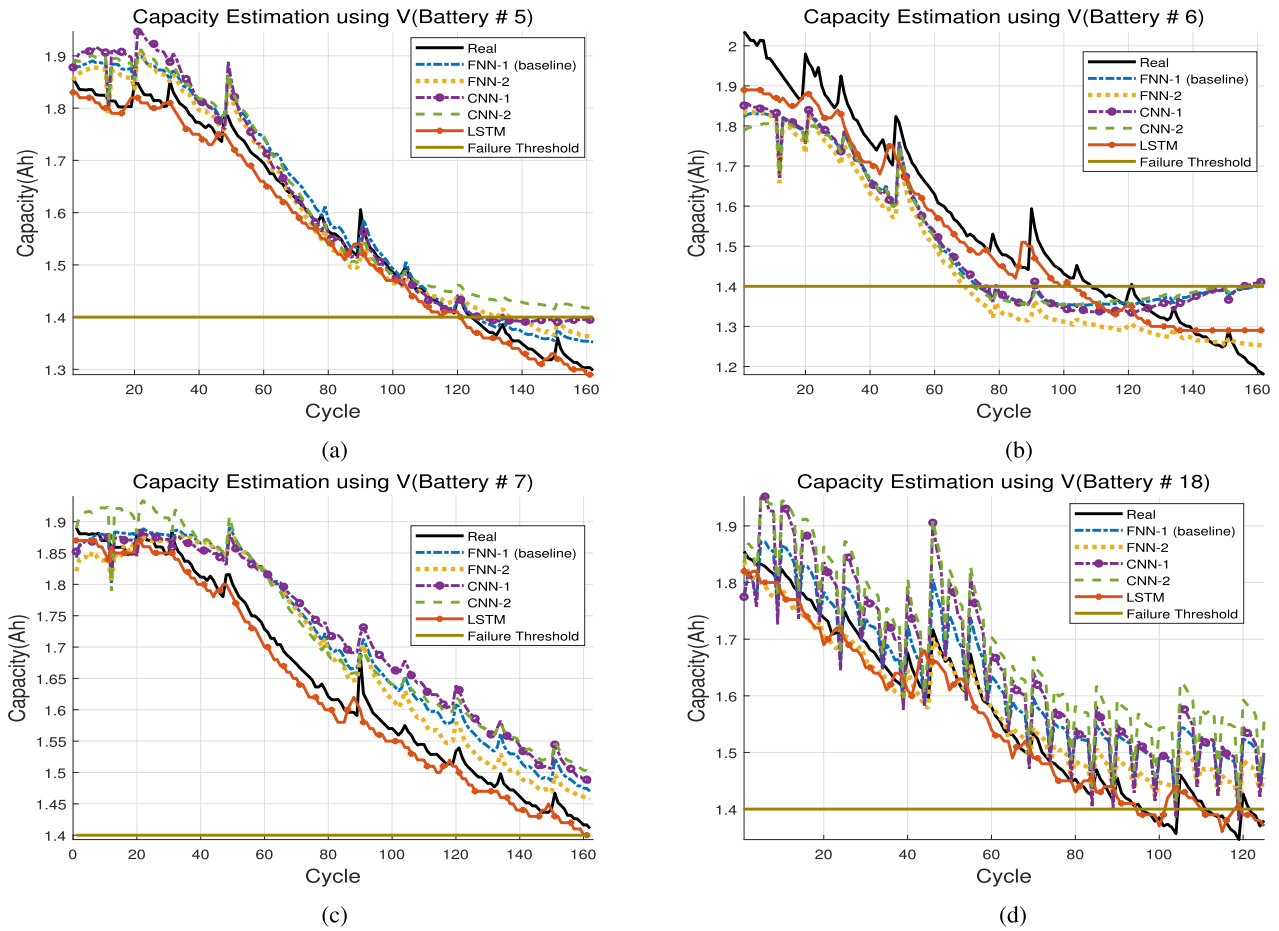


FIGURE 5. Battery capacity estimation based on V data. (a) Battery #5. (b) Battery #6. (c) Battery #7. (d) Battery #18.

TABLE 2. The structures of learning models. FC means fully connected. In CNN, $a \times b @ c$ means c filters with a size of $a \times b$, and the stride is set to (d,d) .

Model	Structure	Num. of Param.
FNN-1	Input-Hidden(10 neurons)-Output (baseline)	Single Ch. : 121 Multi-Ch. : 321
FNN-2	Input-Hidden(40 neurons)-Output Single Ch. : 481 Multi-Ch. : 1,281	
CNN-1	Input-Conv1-Conv2-FC-Output Filter : Conv1($1 \times 2 @ 10$), Conv2($1 \times 2 @ 5$) Stride : Conv1(1,1), Conv2(1,1)	Single Ch. : 186 Multi-Ch. : 226
CNN-2	Input-Conv1-Conv2-FC-Output Filter : Conv1($1 \times 2 @ 30$), Conv2($1 \times 2 @ 15$) Stride : Conv1(1,1), Conv2(1,1)	Single Ch. : 1,156 Multi-Ch. : 1,276
LSTM	Sequence length : 5 Input dimension : 11(Single), 31(Multi)	Single Ch. : 14,740 Multi-Ch. : 17,472

10 neurons in [17] serves as our baseline. We summarize the capacity estimation errors in Table 3 where LSTM shows the substantially better performance than other methodologies. This is because LSTM is good for time series data regression.

TABLE 3. Estimation errors in the case of using V.

Model	RMSE	MAE	MAPE(%)
FNN-1 (baseline)	0.0736	0.0655	4.7100
FNN-2	0.0633	0.0557	3.6500
CNN-1	0.0701	0.0623	4.0020
CNN-2	0.0766	0.0687	4.4187
LSTM	0.0288	0.0210	1.3770

B. ESTIMATION RESULTS OF MULTI-CHANNEL (MC) METHOD

Next we perform the capacity estimation using multi-channel data of voltage, current and temperature charging profiles with 10 uniformly sampled data point per channel. The capacity estimations of the proposed methods are plotted per cycle in Fig. 6. Compared to Fig. 5, it is noticeable that all machine learning methods perform better by using multi-channel charging profiles. For example, in the case of battery #18, the previous high fluctuation and deviation are alleviated. Nevertheless, CNN does not show good

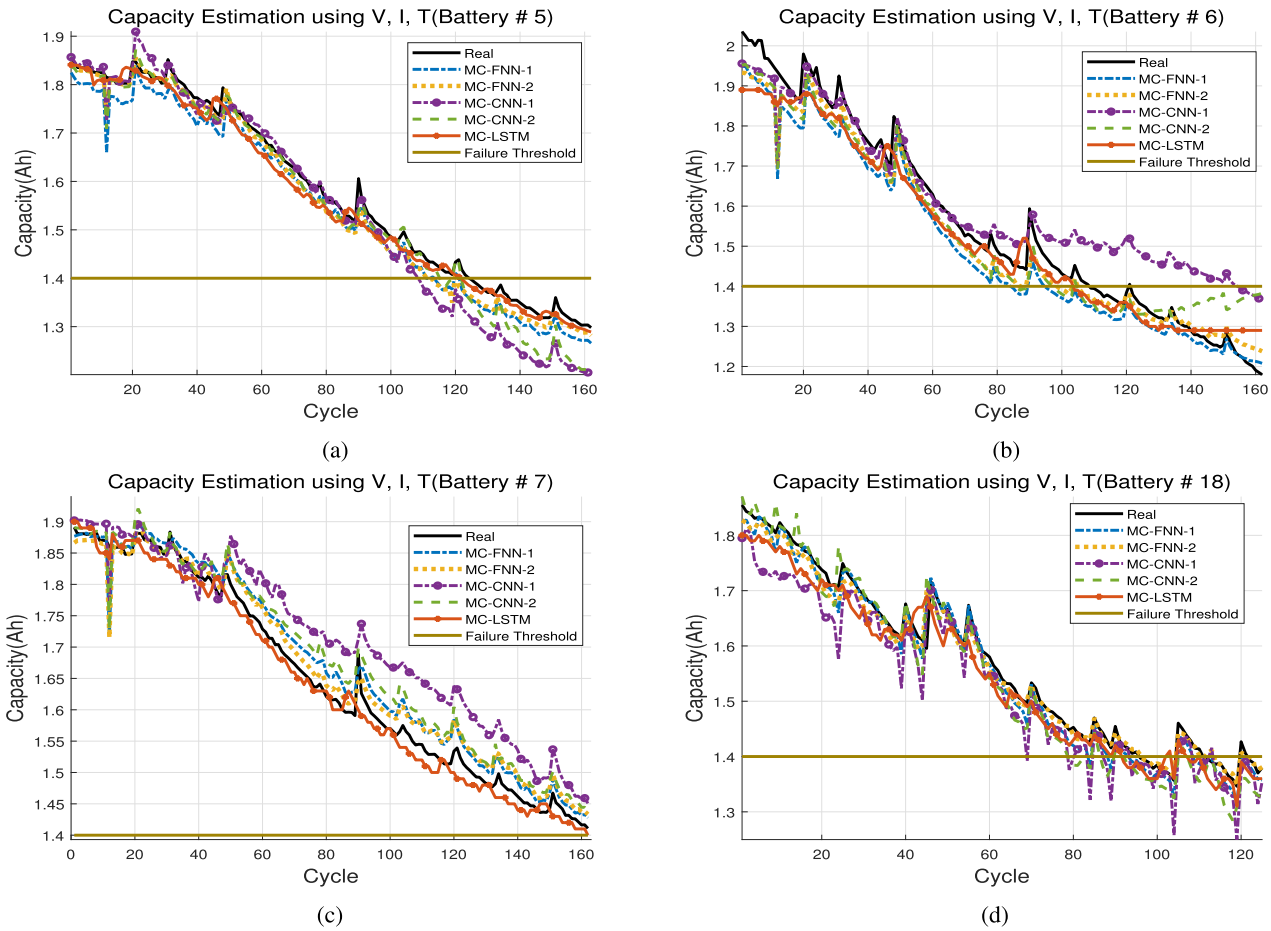


FIGURE 6. Battery capacity estimation based on V, I, T data. (a) Battery #5. (b) Battery #6. (c) Battery #7. (d) Battery #18.

TABLE 4. Estimation errors in the case of using V, I, T.

Model	RMSE	MAE	MAPE(%)
MC-FNN-1	0.0379	0.0329	1.9800
MC-FNN-2	0.0298	0.0242	1.7300
MC-CNN-1	0.0584	0.0443	2.8961
MC-CNN-2	0.0443	0.0364	2.3731
MC-LSTM	0.0246	0.0159	1.0320

performance compared to other methods. We summarize the estimation errors in Table 4, and observe that MC-LSTM shows the best performance among all methodologies as in the case of single channel. In addition all error indices of multi-channel are lower than the cases of single channel, which confirms the diversity of feasible data substantially improves the capacity estimation.

C. MODEL COMPLEXITY VS. ESTIMATION ERROR

Fig. 7 presents the tradeoff between the number of parameters and the estimation error. In the multi-channel case, we

initially expected that MC-CNN would show good performance because having multi-channel charging profiles well matches to multiple convolutional filters well. However, it turns out that MC-CNN is not good for capacity estimation. Specifically, MC-CNN-1 shows the worst error rate compared to other methods even though MC-CNN-1 has the smallest number of parameters. Next we set the numbers of parameters for MC-FNN-2 and MC-CNN-2 similar (i.e., 1,281 and 1,276, respectively) to compare the learning capability of two neural networks. As can be seen in Fig. 7, even though they have similar number of parameters, (i.e., 1,281 and 1,276 respectively), the MAPE of MC-CNN-2 is higher than that of MC-FNN-2 by 0.64 percent point. This confirms that FNN is better than CNN for estimating battery degradation. Furthermore, when the data includes regeneration phenomenon, CNN is not adequate for time series data with high volatility and uncertainty even though CNN is good for other applications such as image recognition.

To quantify the advantage of using multi-channel data, we also compare the performances between MC-FNN-1 and FNN-2 in Fig. 7. Even though MC-FNN-1 has 321 parameters and FNN-2 has 481 parameters, the MAPE of MC-FNN-1 is almost the half of FNN-2. In addition, MC-CNN-1 with

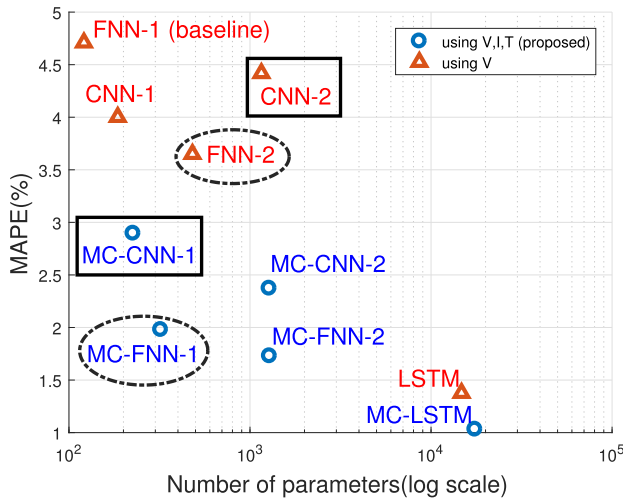


FIGURE 7. Tradeoff between MAPE and the number of parameters.

226 parameters also shows the lower MAPE than CNN-2 with 1,276 parameters as shown in Fig. 7, which confirms the effectiveness of using multi-channel data. However, the more parameters do not necessarily imply the smaller error. For example, even though MC-CNN-2 has 1,276 parameters and MC-FNN-1 has 321 parameters, the MAPE of MC-CNN-2 shows the higher MAPE than MC-FNN-1 as can be seen in Fig. 7.

D. OUTPERFORMANCE OF LSTM

In Figs. 5 and 6, we observe some glitches around 12th cycle; even though the true capacity is not severely low, most learning methods except LSTM estimate the capacity very low. This is because the voltage charging profile at 12th cycle is abnormally deviated from those of other cycles as shown in Fig. 8. We also observe the similar deviations in all four battery charging profiles of current and temperature; these abnormal profiles may be due to measurement noise or sensory malfunction. Consequently, the estimated capacity is far from the true capacity. However, unlike other methods, LSTM estimates the capacity accurately even at the 12th cycle. This is due to the structure of LSTM with memory cell storing long-term information, and this leads to suppress the effect of weight at the 12th cycle data.

E. OUTPERFORMANCE OF THE MULTI-CHANNEL METHOD

In Fig. 9, to demonstrate the outperformance of using V, I, T data, we rearrange the estimation error with respect to battery types. Then, we calculate the difference of MAPE between using V only (dotted) and using V, I, T together (solid). For all four batteries, the single channel FNN-1 (baseline) shows the worst performance on average, which is followed by CNN-2 and CNN-1. LSTM is substantially better than FNN-1, FNN-2, CNN-1, and CNN-2. In all cases we see that multi-channel methods using V, I, T outperform the cases of V irrespective of learning methods. We also observe

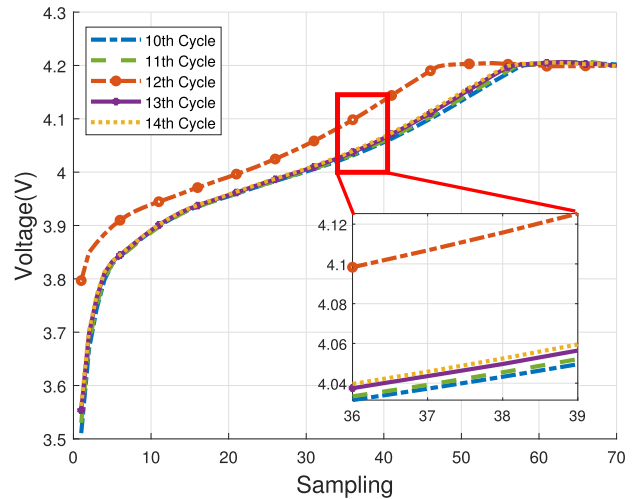


FIGURE 8. Abnormal voltage pattern at 12th cycle of Battery #6.

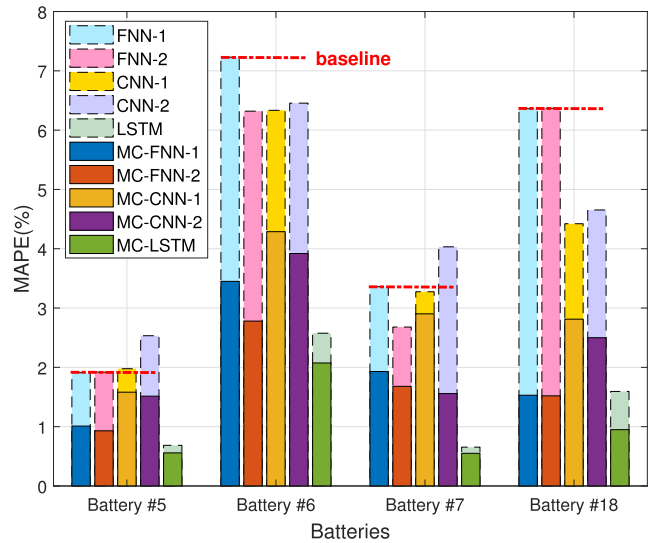


FIGURE 9. MAPE comparison over other methodologies.

that MC-LSTM shows the most accurate estimation in all four batteries.

F. EARLY INDICATION OF EOL

Finally, we investigate the EoL indication and its error. When the measured capacity reaches to 70% (1.4 Ah) of the rated capacity, battery life is declared to be run out. From the viewpoint of PHM, it is more reliable to declare the end of life (EoL) earlier than the actual failure point to secure maintenance time in advance [30], [31]. Note that the EoL is not the first crossover point reaching failure threshold, but the last crossover point considering regeneration phenomenon; reaching failure threshold does not necessarily imply that the battery will no longer function, and indeed the battery may still be usable after rest period. As shown in Table 5, we see that the proposed methods mostly indicate EoL prior to its occurrence (negative values) by using V, I, T data rather than

TABLE 5. EoL indication error.

Battery no. (EoL cycle)	EoL indication error (cycle)		
	V	V, I, T	
Battery #5 (EoL = 125)	FNN-1 (baseline)	+10	MC-FNN-1 -14
	FNN-2	+12	MC-FNN-2 -13
	CNN-1	+10	MC-CNN-1 -16
	CNN-2	N/A	MC-CNN-2 -3
	LSTM	-3	MC-LSTM -3
Battery #6 (EoL = 109)	FNN-1 (baseline)	-17	MC-FNN-1 -14
	FNN-2	-39	MC-FNN-2 -4
	CNN-1	-17	MC-CNN-1 +46
	CNN-2	-37	MC-CNN-2 -4
	LSTM	-5	MC-LSTM -5
Battery #7	N/A		N/A
Battery #18 (EoL = 122)	FNN-1 (baseline)	+2	MC-FNN-1 -13
	FNN-2	N/A	MC-FNN-2 0
	CNN-1	+2	MC-CNN-1 -8
	CNN-2	N/A	MC-CNN-2 -14
	LSTM	+2	MC-LSTM -11

only using V, which is helpful for reliable and safe battery operation.

V. CONCLUSION

In this paper, we proposed a capacity estimation framework for lithium-ion battery based on FNN, CNN and LSTM with multi-channel V, I, T data. By utilizing lithium-ion battery dataset of NASA, we have analyzed the estimation results from the perspective of error indices and capacity difference per cycle as well. Numerical results demonstrated that the diversity of feasible data is critical for the estimation with high accuracy. In particular, we showed that the proposed multi-channel method outperforms the existing method with only single voltage data by up to 58%, 46% and 25% of MAPE improvement in the case of FNN, CNN and LSTM, respectively. In future work, the proposed method can be extended by considering an online method which adaptively updates the internal parameters of physics-based equations affecting actual degradation in real-time practical operation.

REFERENCES

- [1] Z. Liu, Z. Jia, C.-M. Vong, J. Han, C. Yan, and M. Pecht, "A patent analysis of prognostics and health management (PHM) innovations for electrical systems," *IEEE Access*, vol. 6, pp. 18088–18107, 2018.
- [2] B. Saha, K. Goebel, S. Poll, and J. Christophersen, "Prognostics methods for battery health monitoring using a Bayesian framework," *IEEE Trans. Instrum. Meas.*, vol. 58, no. 2, pp. 291–296, Feb. 2009.
- [3] *Condition Monitoring and Diagnostics of Machines Prognostics Part1: General Guidelines*, Int. Standards Organisation, Geneva, Switzerland, Nov. 2004.
- [4] J. Meng, D.-L. Stroe, M. Ricco, G. Luo, and R. Teodorescu, "A simplified model-based state-of-charge estimation approach for lithium-ion battery with dynamic linear model," *IEEE Trans. Ind. Electron.*, vol. 66, no. 10, pp. 7717–7727, Oct. 2019.
- [5] D.-I. Stroe, V. Knap, M. Swierczynski, A.-I. Stroe, and R. Teodorescu, "Operation of a grid-connected lithium-ion battery energy storage system for primary frequency regulation: A battery lifetime perspective," *IEEE Trans. Ind. Appl.*, vol. 53, no. 1, pp. 430–438, Jan./Feb. 2017.
- [6] K. Goebel, B. Saha, A. Saxena, J. R. Celaya, and J. P. Christophersen, "Prognostics in battery health management," *IEEE Instrum. Meas. Mag.*, vol. 11, no. 4, pp. 33–40, Aug. 2008.
- [7] M. Daigle and C. S. Kulkarni, "End-of-discharge and end-of-life prediction in lithium-ion batteries with electrochemistry-based aging models," in *Proc. AIAA Infotech@ Aerosp.*, Jan. 2016, p. 2132.
- [8] M. Safari and C. Delacourt, "Simulation-based analysis of aging phenomena in a commercial graphite/LiFePO₄ Cell," *J. Electrochim. Soc.*, vol. 158, no. 12, pp. A1436–A1447, Jan. 2011.
- [9] D. Liu, X. Yin, Y. Song, W. Liu, and Y. Peng, "An on-line state of health estimation of lithium-ion battery using unscented particle filter," *IEEE Access*, vol. 6, pp. 40990–41001, Jul. 2018.
- [10] G. L. Plett, "Extended Kalman filtering for battery management systems of LiPB-based HEV battery packs: Part 3. State and parameter estimation," *J. Power Sources*, vol. 134, no. 2, pp. 277–292, 2004.
- [11] A. Guha and A. Patra, "State of health estimation of lithium-ion batteries using capacity fade and internal resistance growth models," *IEEE Trans. Transp. Electrific.*, vol. 4, no. 1, pp. 135–146, Mar. 2018.
- [12] E. Walker, S. Rayman, and R. E. White, "Comparison of a particle filter and other state estimation methods for prognostics of lithium-ion batteries," *J. Power Sources*, vol. 287, pp. 1–12, Aug. 2015.
- [13] X. Zheng and H. Fang, "An integrated unscented Kalman filter and relevance vector regression approach for lithium-ion battery remaining useful life and short-term capacity prediction," *Rel. Eng. Syst. Safety*, vol. 144, pp. 74–82, Dec. 2015.
- [14] M. A. Patil, P. Tagade, K. S. Hariharan, S. M. Kolake, T. Song, T. Yeo, and S. Doo, "A novel multistage support vector machine based approach for Li ion battery remaining useful life estimation," *Appl. Energy*, vol. 159, pp. 285–297, Dec. 2015.
- [15] Y. Li, S. Zhong, Q. Zhong, and K. Shi, "Lithium-ion battery state of health monitoring based on ensemble learning," *IEEE Access*, vol. 7, pp. 8754–8762, Jan. 2019.
- [16] D. Liu, J. Zhou, H. Liao, Y. Peng, and X. Peng, "A health indicator extraction and optimization framework for lithium-ion battery degradation modeling and prognostics," *IEEE Trans. Syst., Man, Cybern. Syst.*, vol. 45, no. 6, pp. 915–928, Jun. 2015. doi: 10.1109/TSMC.2015.2389757.
- [17] J. Wu, C. Zhang, and Z. Chen, "An online method for lithium-ion battery remaining useful life estimation using importance sampling and neural networks," *Appl. Energy*, vol. 173, pp. 134–140, Jul. 2016.
- [18] G.-W. You, S. Park, and D. Oh, "Diagnosis of electric vehicle batteries using recurrent neural networks," *IEEE Trans. Ind. Electron.*, vol. 64, no. 6, pp. 4885–4893, Jun. 2017.
- [19] X. Hu, J. Jiang, D. Cao, and B. Egardt, "Battery health prognosis for electric vehicles using sample entropy and sparse Bayesian predictive modeling," *IEEE Trans. Ind. Electron.*, vol. 63, no. 4, pp. 2645–2656, Apr. 2016.
- [20] B. Saha and K. Goebel, "Battery data set," NASA AMES Prognostics Data Repository, 2007.
- [21] M. Rashid and A. Gupta, "Effect of relaxation periods over cycling performance of a Li-ion battery," *J. Electrochim. Soc.*, vol. 162, no. 2, pp. A3145–A3153, Jan. 2015.
- [22] L. He, G. Meng, Y. Gu, C. Liu, J. Sun, T. Zhu, Y. Liu, and K. G. Shin, "Battery-aware mobile data service," *IEEE Trans. Mobile Comput.*, vol. 16, no. 6, pp. 1544–1558, Jun. 2017.
- [23] A. Jain, K. Nandakumar, and A. Ross, "Score normalization in multimodal biometric systems," *Pattern Recognit.*, vol. 38, no. 12, pp. 2270–2285, Dec. 2005.
- [24] I. Goodfellow, Y. Bengio, and A. Courville, *Deep Learning*. Cambridge, MA, USA: MIT Press, 2016. [Online]. Available: <http://www.deeplearningbook.org>
- [25] H. Choi, S. Ryu, and H. Kim, "Short-Term load forecasting based on ResNet and LSTM," in *Proc. IEEE Int. Conf. Commun., Control, Comput. Technol. Smart Grids (SmartGridComm)*, Oct. 2018, pp. 1–6.
- [26] S. Hochreiter and J. Schmidhuber, "Long short-term memory," *Neural Comput.*, vol. 9, no. 8, pp. 1735–1780, 1997.
- [27] M. Abadi, P. Barham, J. Chen, Z. Chen, A. Davis, J. Dean, M. Devin, S. Ghemawat, G. Irving, M. Isard, and M. Kudlur, "Tensorflow: A system for large-scale machine learning," in *Proc. 12th USENIX Symp. Operating Syst. Design Implement. (OSDI)*, Nov. 2016, pp. 265–283.
- [28] D. P. Kingma and J. Ba, "Adam: A method for stochastic optimization," in *Proc. Int. Conf. Learn. Represent. (ICLR)*, May 2015, pp. 1–13.
- [29] A. L. Maas, A. Y. Hannun, and A. Y. Ng, "Rectifier nonlinearities improve neural network acoustic models," in *Proc. Int. Conf. Mach. Learn.(ICML)*, Jun. 2013, vol. 30, no. 1, pp. 1–6.
- [30] T. Wang, J. Yu, D. Siegel, and J. Lee, "A similarity-based prognostics approach for Remaining Useful Life estimation of engineered systems," in *Proc. Int. Conf. Prognostics Health Manage.*, Oct. 2008, pp. 1–6.

- [31] C. Kunlong, J. Jiuchun, Z. Fangdan, S. Bingxiang, and Z. Yanru, "SOH estimation for lithium-ion batteries: A cointegration and error correction approach," in *Proc. IEEE Int. Conf. Prognostics Health Manage. (ICPHM)*, Jun. 2016, pp. 1–6.



YOHWAN CHOI received the B.S. and Ph.D. degrees in electronic engineering from Sogang University, in 2013 and 2019, respectively. His research interests include the state of health estimation, smart battery management, energy storage systems, and power economics and optimization.



SEUNGHYOUNG RYU received the B.S. and M.S. degrees in electronic engineering from Sogang University, in 2014 and 2016, respectively. He is currently pursuing the Ph.D. degree with the Department of Electronic Engineering, Sogang University, South Korea. His research interests include transactive energy, energy data analysis, energy forecasting, machine learning, and artificial intelligence in the smart grid.



KYUNGNAM PARK received the B.S. degree in electronic engineering from Sogang University, in 2017. He is currently pursuing the M.S. degree with the Department of Electronic Engineering, Sogang University, South Korea. His research interests include energy analytics, recurrent neural networks, load forecasting, and generative adversarial networks. He was a recipient of the Full Scholarship for Excellent Undergraduate GPA, in 2017, and CSAT Math and Science Scores from the Department of Electronic Engineering, Sogang University, in 2012, respectively.



HONGSEOK KIM (S'06–M'10–SM'16) received the B.S. and M.S. degrees in electrical engineering from Seoul National University, in 1998 and 2000, respectively, and the Ph.D. degree in electrical and computer engineering from The University of Texas at Austin, in 2009. He was a Member of Technical Staff with Korea Telecom Labs, from 2000 to 2005. He was a Postdoctoral Research Associate with the Department of Electrical Engineering, Princeton University, from 2009 to 2010.

He was a Member of Technical Staff with Bell Labs, USA, from 2010 to 2011. He is currently an Associate Professor with the Department of Electronic Engineering, Sogang University, South Korea. His research interests include smart grid and energy ICT, specifically focused on machine learning for energy forecasting, energy trading and electricity market, energy storage systems, microgrid, optimal power flow, and wireless networks. He was a recipient of the Korea Government Overseas Scholarship, from 2005 to 2008. He received the Haedong Young Professional Award, in 2016. He served as an Editor of the *Journal of Communications and Networks* and the Guest Editor of *Energies* with the special issue of Machine Learning and Optimization with Applications of Power System.

• • •